J. Fluid Mech. (1973), *vol.* 57, *part* 3, *pp.* 549–582
Printed in Great Britain

Conditional sampling and other measurements in a plane turbulent wake

By R. M. THOMAS†
Cavendish Laboratory, University of Cambridge

(Received 3 July 1972)

A series of hot-wire measurements has been carried out in a plane wake to investigate the structure of the turbulence boundary and the relation of its instantaneous position to the behaviour in the core of the flow. The principal measured quantities are as follows: mean velocity profile; intermittency factor; burst rate; mean of the longitudinal component of velocity conditioned upon various specified interface positions; autocorrelation of the intermittency signal; probability densities at the half-intermittency point for the time between bursts and the duration of a burst; probability density for the longitudinal velocity component and its time derivative at various points across the wake; probability density at the half-intermittency point for the same quantities in the turbulent and irrotational zones separately. In addition, the profile of the second moment of the probability density for the time between bursts has been obtained indirectly and part of the theory of Phillips (1955) has been shown to be applicable in the intermittent region.

The present measurements appear to indicate that the turbulence boundary in the wake resembles that in other plane flows more closely than has been supposed hitherto. The theory of normally distributed random noise was found to explain many of the observed statistical properties of the turbulence boundary.

1. Introduction

The basic structure of the plane wake has been well established by the extensive early experiments of Townsend (1947, 1948, 1949*a*, *b*), but in recent years the view has been increasingly expressed that many interesting features of turbulent flow are concealed by restricting measurements to long-time averages. The work of Kovasznay, Kibens & Blackwelder (1970) and Wygnanski & Fiedler (1970) has illustrated the usefulness of developing new averaging methods in which samples are conditioned upon the instantaneous position of the moving interface between turbulent and irrotational zones, sometimes called the turbulence boundary. The work reported here represents an application and extension of these techniques in a re-examination of some aspects of the plane wake.

A first step in investigating the structure of the turbulence boundary is the definition of an intermittency factor as the average proportion of time that the turbulent condition exists at a given point in the flow. The profile of this quantity

† Present address: Central Electricity Research Laboratories, Leatherhead, Surrey.

may be conveniently obtained by constructing an electronic circuit which processes the anemometer signal to yield an output that is unity in the presence of turbulence and zero otherwise. Such a device is known as a turbulence detector and its output will be called the intermittency signal. The intermittency factor may be obtained directly by smoothing the output of the turbulence detector.

Once a turbulence detector has been built, a number of other interesting measurements become possible. By differentiating the intermittency signal and feeding the resulting pulses to an electronic counter the average rate at which the interface intersects the detector probe can be determined. This is an important quantity which will be called the burst rate. The pulses may also be used to operate a circuit which samples another signal representing a fluctuating flow parameter obtained from a hot-wire probe at a different location. This technique, originally suggested by Betchov & Criminale (1964) and known as conditional sampling, enables a picture to be built up of the flow conditions associated with a specified interface position. The intermittency signal may alternatively be used to gate a second signal directly. For example, by gating the signal from the same anemometer that drives the turbulence detector and smoothing the output, the mean velocity in the turbulent zone may be found separately; this type of measurement is called zone averaging to distinguish it from the conditional sampling described above. If the gated signal is fed to a probability analyser it is possible to obtain zone probability densities, although the number of moments which can be meaningfully extracted is strongly dependent upon the efficiency of the turbulence detector.

The following co-ordinate system will be used: x is the downstream direction, y is the direction of largest gradients of mean values and z is the direction in which the flow is homogeneous. No attempt has been made to present the experimental data in non-dimensional form, since it is felt that this practice tends to obscure the difficulties associated with finite probe size, limited frequency response of the instrumentation, etc. In order to render the results dimensionless it is necessary only to note that the local length and velocity scales are as follows: distance of half-intermittency point from wake centre = 54 mm; peak mean velocity defect = 0·80 m/s.

2. Apparatus and instrumentation

2.1. *Wind tunnel*

The experiments were carried out in a small closed-return wind-tunnel at the Cavendish Laboratory. The working section has a useful length of about 2 m and a cross-section at the entrance of 0·38 × 0·38 m, increasing slightly with downstream distance to compensate for boundary-layer growth. A contraction of approximately 9 : 1 precedes the working section and the r.m.s. longitudinal turbulence intensity is less than 0·07 % at a speed of 10 m/s. Screens are fitted to clean the circulating air.

The wake-forming body was a metal cylinder 9·58 mm in diameter mounted horizontally in the working section immediately after the contraction. The free-stream speed was monitored by means of a manometer permanently connected

across the contraction. Except for a few tests, the speed was maintained within 1 % of 10 m/s throughout the series of experiments, the corresponding Reynolds number based on cylinder diameter being 6600. All the hot-wire measurements were made at a station 1·52 m behind the cylinder, i.e. very nearly 160 diameters downstream.

2.2. *Anemometers*

Two simple constant-temperature anemometers were designed and built. Some difficulty was encountered in the development of a stable circuit; an account of the problems and their eventual solution, together with full circuit details of the anemometers and the other equipment described below, are given by Thomas (1971).

Almost all the measurements were carried out with Wollaston wires typically 0·3–0·6 mm in length and with cold resistances between 10 and 20 ohms. Calculated length-to-diameter ratios were in the range 160–220; no corrections for wire length were made. A few tests were made with a DISA miniature hot-wire probe type 55 A 25. Nominal overheat ratios of 0·8 and 0·5 were used.

The anemometer bandwidth was measured by injecting a square-wave current into the bridge while the hot-wire was supported in a steady air-stream at 10 m/s (obtained by temporarily removing the cylinder from the working section). The Wollaston wires gave results in the range 15–40 kHz, depending on the particular wire used and, of course, the overheat ratio. No attempt was made to match the anemometers to the DISA wire, with the result that this gave a bandwidth of 2–3 kHz and an underdamped response.

The wires were calibrated in the wind tunnel (with the cylinder again removed) against a pitot-static tube and micromanometer over a speed range of 6–12 m/s. The wires were operated at fixed resistance. A simple calculation shows that in the present wake flow the nonlinearity of the relation between voltage and velocity leads to less than 1·5 % second harmonic distortion in the turbulence signal and is insufficient to cause significant difference between the static sensitivity and the effective sensitivity in the presence of a fluctuating component of bridge voltage. It is also easily shown that the sensitivity is 4 % higher in the centre of the wake, which has a peak velocity defect of 8 %, than in the free stream. A correction for this was included in the computer programs written to reduce the experimental results.

2.3. *Turbulence detector*

The turbulence detector was designed to use a relatively narrow frequency band of the longitudinal velocity fluctuation as the basic indicator. This technique will be successful if, first, the fluctuations in the irrotational fluid have negligible components in the band used and, second, components in the band are continuously present in the turbulent zone. After a number of tests a band centred at 1 kHz was adopted, this being the highest value that could be used without encountering the problems associated with electrical noise. The band-pass effect was simply achieved by passing the anemometer signal through a multistage pre-amplifier with carefully designed coupling networks; the ultimate

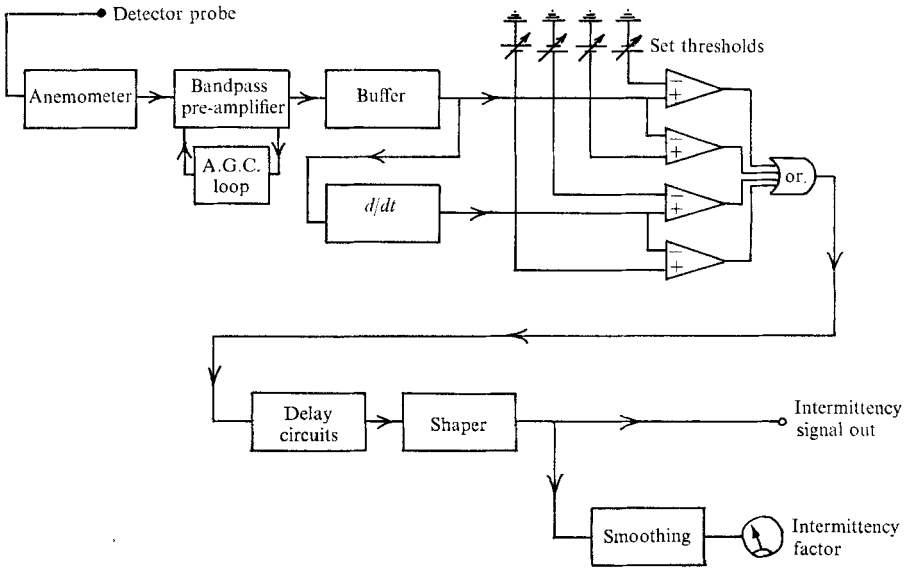

FIGURE 1. Turbulence detector.

roll-off was 24 dB/octave on each side. The pre-amplifier was also provided with automatic gain control, which kept the output at a suitable level regardless of the position of the hot wire within the wake. In this way it was possible to eliminate the necessity of making adjustments to the detector circuits each time the probe was moved. The output of the pre-amplifier consisted of bursts of oscillations at about 1 kHz while the probe was in turbulence. This train of bursts was then fed to a trigger circuit which converted it into a square-wave signal. The design of the trigger is much easier when it is required to deal only with bursts of a fixed frequency than when it is fed directly with turbulence or a derivative; it is largely for this reason that the narrow-band filtering system described above was developed.

A block diagram of the complete system is shown in figure 1. The burst-train is full-wave rectified by a pair of limiting amplifiers with separately adjustable thresholds. The bursts are also differentiated, the result rectified in the same way and the outputs of the four limiters fed to an or-gate. The purpose of the differentiating channel is to bridge the zeros of the straight-through channel, the effect being similar to that of the phase-shift technique described by Fiedler & Head (1966). The output of the or-gate is somewhat jittery and needs smoothing to eliminate spurious responses. This is performed by an active network which may be adjusted to give equal attack and decay times. The signal is then shaped by a limiter, part of the shaped output being smoothed by a passive low-pass filter and used to drive a moving-coil meter, which thus provides a direct read-out of intermittency factor.

The various initial adjustments were made by a process of trial and error, oscillograms being used to evaluate performance. It was found that good results could be achieved only at the expense of rather long attack and decay times, typically of the order of 2 ms. This effect, which is also observed in turbulence

detectors based on differentiated signals, seems to be connected with the intermittent structure of the small scales of turbulence discussed by Batchelor & Townsend (1949) and Sandborn (1959); it is not to be confused with the inherent uncertainty (about 0·03 ms in the present case) arising from the finite thickness of the turbulence boundary. The apparently inevitable 2 ms lag is a rather serious problem in certain measurements, but can be partially overcome by advancing the detector probe in the upstream direction by the appropriate amount (i.e. 20 mm at a free-stream speed of 10 m/s). If the shape of the turbulence boundary persists as it is convected downstream, as is suggested by the space–time correlation of the intermittency signal reported by Kovasznay *et al.* (1970), then it might be expected that the signal obtained from a spatially advanced probe approximates the signal that would be obtained from a probe at the original location used in conjunction with an ideal turbulence detector. This technique has been used for all the experiments described below, but it cannot be said to be entirely satisfactory in view of the degree of ambiguity it introduces into the interpretation of the data.

2.4. *Sampling correlator*

Differentiation of the random square wave from the turbulence detector yields a train of short pulses, each of which marks an instant at which the detector probe enters or leaves the turbulent zone. These pulses could be shaped and used directly to gate a signal from another anemometer to give, after smoothing, the conditional mean velocity. However, this system has the disadvantage of limited range, since measurements are possible only where the burst rate is high enough to prevent the smoothed pulse train representing the conditional mean from being lost in the drift associated with the subsequent d.c. amplification. A different technique has been used for the present experiments. The pulses are used to operate a sample-and-hold system in which the hold time is much longer than the average time between pulses at the half-intermittency point. Pulses received while holding are ignored and when the hold time has elapsed the circuits are promptly reset, ready for the next pulse. The sequence of samples is smoothed to give the required average. The conditional mean velocity measured in this way differs slightly from that obtained by the first method described above; the relationship between the two types of measurement will be discussed in §4.2. With careful circuit design the sample-and-hold system can provide a sensitivity significantly greater than that attainable with the direct approach. The equipment described here has been used successfully with the detector probe at locations where the intermittency factor was below 0·01 or greater than 0·99.

A block diagram of the sampling correlator appears in figure 2. The signal from the anemometer is first passed through an amplifier whose bandwidth is restricted to 0·1 Hz to 5 kHz in order to improve the signal-to-noise ratio. The amplified signal is fed to a follower which normally drives a small capacitor. When a pulse arrives from the turbulence detector this capacitor is immediately isolated from its driver and retains the voltage on it at the moment of sampling for 1·4 ms. During this period a second follower charges a much larger capacitor

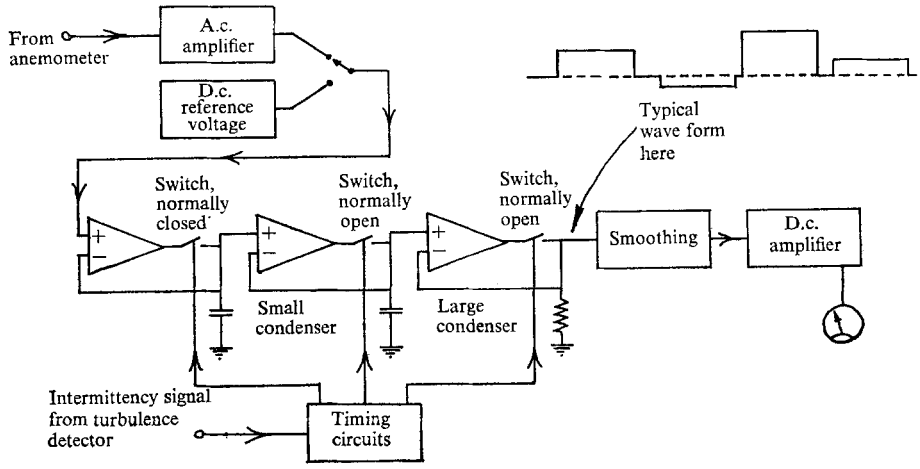

FIGURE 2. Sampling correlator. The switches operated by the timing circuits are diode gates.

to the same voltage, a process which requires large currents and cannot be carried out instantaneously. When the voltage has been transferred to the large capacitor this too is isolated and allowed accurately to retain its charge for 92 ms. The voltage stored on the large capacitor is reproduced at low impedance by a further follower provided with a gate which permits the output to fall to zero when the 92 ms hold time has elapsed. The use of a two-stage holding system is dictated by the conflicting requirements of a long overall hold time and adequate frequency response. The present equipment is capable of following the incoming anemometer signal and can also hold samples of up to 2 V within a few millivolts for $\frac{1}{2}$ s or more, although a smaller hold time was actually used in order to have a higher sampling rate. The form of the output of the third gate is also shown in figure 2. Between samples the output is clamped to zero, the proportion of dead time being dependent on the burst rate, and it is necessary to correct for this if a simple sample average is required. The ratio of total time to the time during which samples are actually present will be called the weighting factor; it is easily measured by disconnecting the anemometer signal and feeding a known steady voltage through the sampling system while continuing to use the same signal from the turbulence detector. Facilities for this measurement were built into the sampling correlator. The wave form of figure 2 is finally smoothed and after d.c. amplification the output is displayed on a moving-coil meter.

A series of tests was carried out to investigate the performance of the equipment. It was found that errors due to spurious electrical signals generated within the correlator were equivalent to an uncertainty in flow velocity of about 2·5 mm/s, or 1 % of the r.m.s. longitudinal turbulence intensity at the centre of the wake.

2.5. *Probability analyser and other equipment*

The block diagram shown in figure 3 is largely self-explanatory. The r.m.s. amplitude sent to the analyser was of the order of $\frac{1}{2}$V, whereas the minimum window width available was 11·1 mV. Measurement of probability densities in

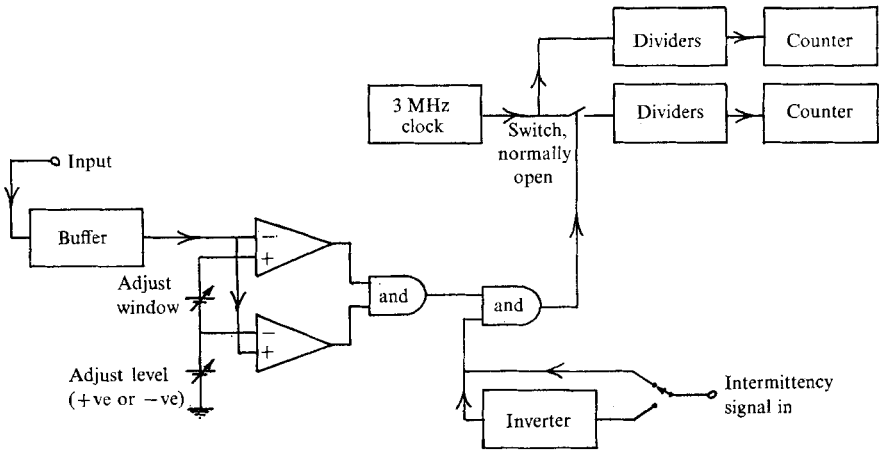

FIGURE 3. Probability analyser.

the turbulent and irrotational zones separately was made possible by the inclusion of a gate operated by the intermittency signal from the turbulence detector. When the equipment was operated in this mode clock pulses were allowed through to the counter only when the input signal was in the correct range and the intermittency signal simultaneously indicated the specified type of flow. Tests carried out to investigate the effect of using different windows to measure the probability densities of actual turbulent signals confirmed that the clock frequency was sufficiently high.

Permanent records of the anemometer and intermittency signals were made with aid of a C.E.C. type 5-124 ultraviolet recording oscillograph, using galvanometers with a response flat ($\pm 5\,\%$) to 1·2 kHz. Differentiation of turbulence signals was performed by a DISA random signal indicator and correlator type 55A06, followed by a passive low-pass filter with a cut-off at 10 kHz. A simple d.c. amplifier with large adjustable offset was built to permit hot-wire measurements of the mean velocity profile by backing off most of the anemometer bridge voltage.

3. Experimental procedure and results

3.1. *Preliminary checks*

The pressure gradient along the wake was measured by using the pressure-tapping holes provided in the roof and floor of the wind-tunnel; the results obtained are shown in figure 4. It is clear that between the cylinder and the station at which the remaining measurements were carried out the flow was subjected to a negligible pressure gradient.

Two-dimensionality of the wake was investigated by measuring with a pitot-static tube and micromanometer the peak velocity defect in the wake 1·52 m behind the cylinder for various values of z, the co-ordinate parallel to the cylinder axis. As a further check, the r.m.s. longitudinal turbulence intensity on the wake centre-plane was measured (using the probability analyser) for several

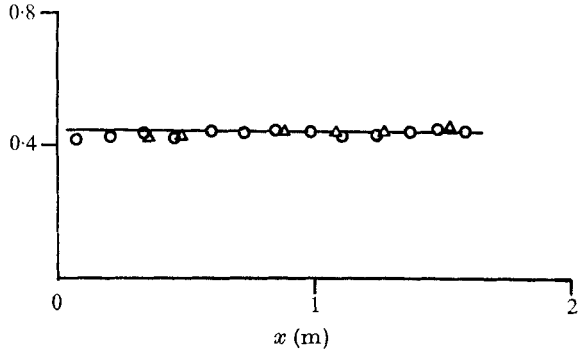

FIGURE 4. Ratio of static pressure (relative to atmospheric) to dynamic head at 10 m/s plotted against downstream distance. ○, pressure-tapping holes on roof of tunnel; △, pressure-tapping holes on floor of tunnel.

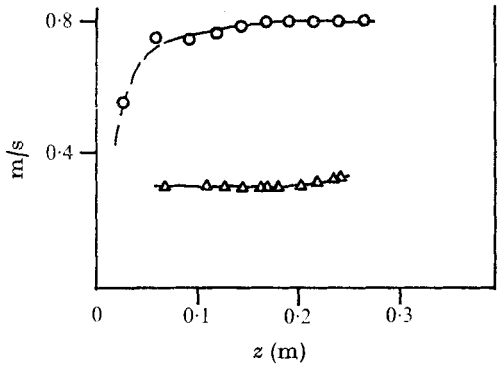

FIGURE 5. Two-dimensionality. ○, peak mean velocity defect; △, r.m.s. longitudinal turbulence intensity on the wake centre-plane.

different values of z. The results are plotted in figure 5. The measurements of turbulence intensity involved the movement of the rather bulky downstream traversing gear across the tunnel; the varying blockage may account for the apparent rise in turbulence intensity as the back wall of the tunnel is approached. This explanation is supported by the homogeneity of the mean velocity defect, which was measured with the pitot-static tube inserted through a tunnel wall and hence involved no alteration of the position of the traversing gear.

3.2. *Mean velocity profile*

A direct measurement of the mean velocity profile with a total-head tube proved to be difficult owing to small short-term variations in tunnel speed, so a second total-head tube was introduced into the free stream, well outside the wake, and used to back off the micromanometer. In this way, reproducible results could be obtained, although some care was necesary to avoid errors due to temperature drift. The profile of mean velocity is shown in figure 6. The slight asymmetry, which was reproduced in a series of tests involving total-head tubes of various diameters and several different locations of the back-off tube, is thought to be another consequence of blockage by the traversing gear. The profile obtained

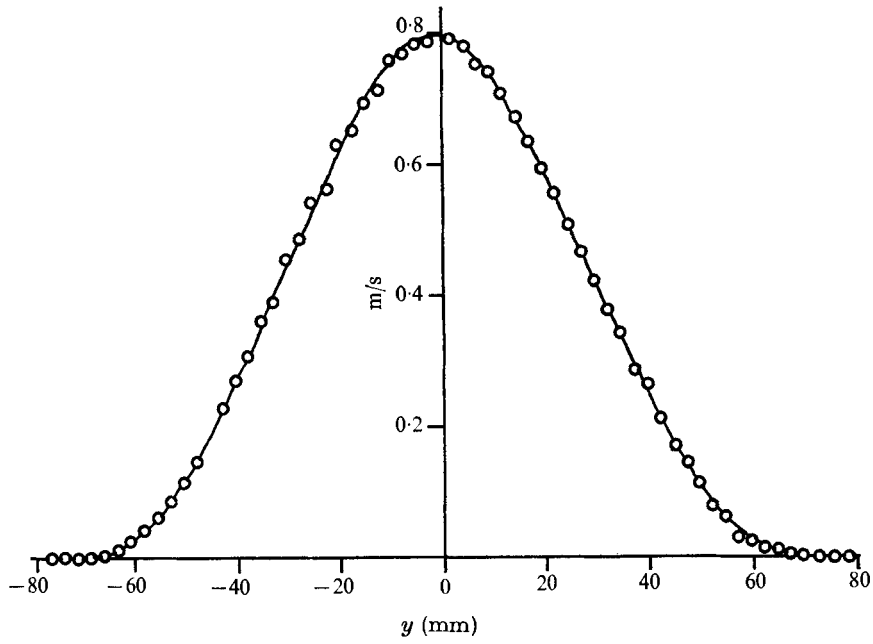

FIGURE 6. Mean velocity profile.

with the pair of total-head tubes was checked by means of a hot-wire anemometer connected to a d.c. amplifier with facilities for backing off most of the bridge voltage. The hot-wire data displayed considerable scatter, but no systematic deviation from the profile of figure 6 could be found. The present peak defect and wake width are within 3 % of the results obtained by Townsend (1949*a*) in a very similar flow.

3.3. *Intermittency factor and burst rate*

The turbulence detector provides a direct read-out of intermittency factor and the burst rate can be measured by feeding the intermittency signal for a known period to an electronic counter sensitive to (say) negative-going edges. Profiles of the two quantities are presented in figure 7. A counting period of 50 s was used for the burst-rate measurements. The results display better symmetry about the centre-plane than does the mean velocity.

The profile of intermittency factor is well approximated by an error curve with a standard deviation of 11·4 mm, centred at 53·8 mm from the centre of the wake, although small systematic differences can be discerned. An attempt has been made in figure 7 to fit the burst rate by a Gaussian distribution with a standard deviation equal to that of the error curve. It would appear that, in spite of the noticeable non-Gaussianity of the burst-rate profile, its standard deviation is not very different from that of the intermittency factor. The significance of this fact will be discussed in §4.1.

The curves shown in figure 7 were checked a number of times over a period of several months and found to be surprisingly reproducible. The uncertainty in intermittency factor at a given point did not exceed $\pm 0{\cdot}04$, and the burst-rate

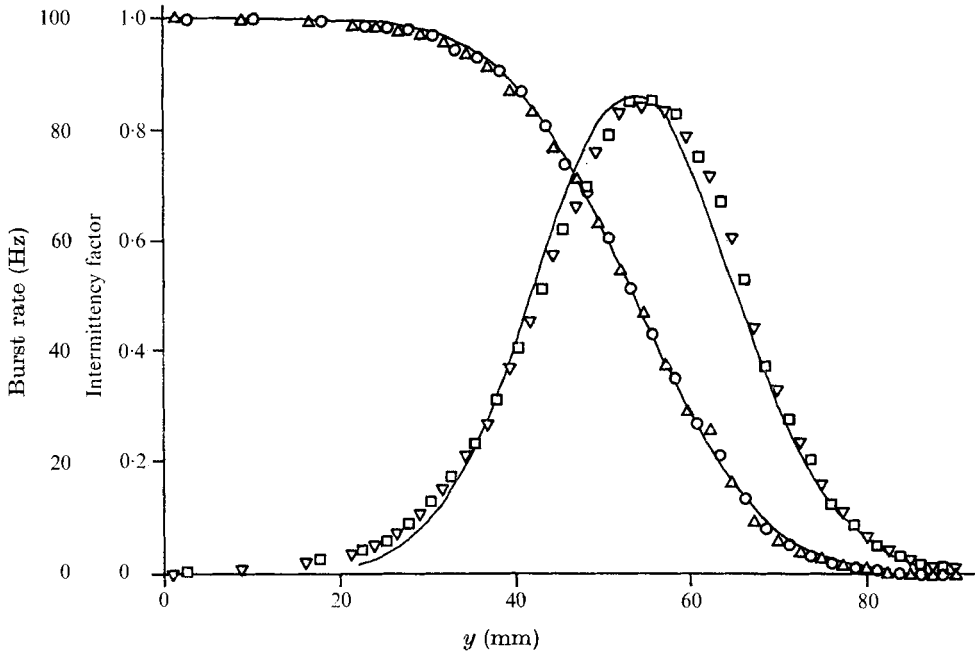

FIGURE 7. Intermittency factor and burst rate. ○, □, $y > 0$; △, ▽, $y < 0$. The intermittency factor is fitted by

$$\frac{1}{2} - \frac{1}{(2\pi)^{\frac{1}{2}}} \int_0^{(y-y_0)/\sigma_0} e^{-\frac{1}{2}t^2}\, dt,$$

and the burst rate is fitted by $86 \exp[-(y-y_0)^2/2\sigma_0^2]$. In both cases $y_0 = 53{\cdot}8$ mm; $\sigma_0 = 11{\cdot}4$ mm.

uncertainty was less than ± 5 Hz. The corresponding error in the position of the half-intermittency point is about ± 2 %. From time to time the thresholds of the turbulence detector required slight adjustment, the procedure being the same as that used in initially setting up the circuits. Therefore the degree of repeatability indicated by the figures quoted above may be regarded as reflecting the consistency, over a period, of the criteria used to evaluate the oscillograms. It is more difficult to place limits on the possible systematic errors associated with the subjective nature of the adjustment procedure itself. Although a complete investigation of effect of thresholds and smoothing times was not attempted owing to the large number of independent adjustable parameters involved, observations indicated that when the inevitable subjectivity is included as a source of error the uncertainties in the intermittency factor and the position of the half-intermittency point are not more than twice the estimates given above, while the burst rate is somewhat less reliable. For example, in a preliminary stage of its development the turbulence detector was adjusted to give a peak burst rate of 120 Hz; in this condition the response is quite jittery, but the output still corresponds recognizably to the intermittent structure of the anemometer signal. Compared with figure 7 the intermittency factor obtained with this detector had a practically unchanged standard deviation, and the half-intermittency point was only 5 % further from the centre-plane of the wake. It may be concluded that the

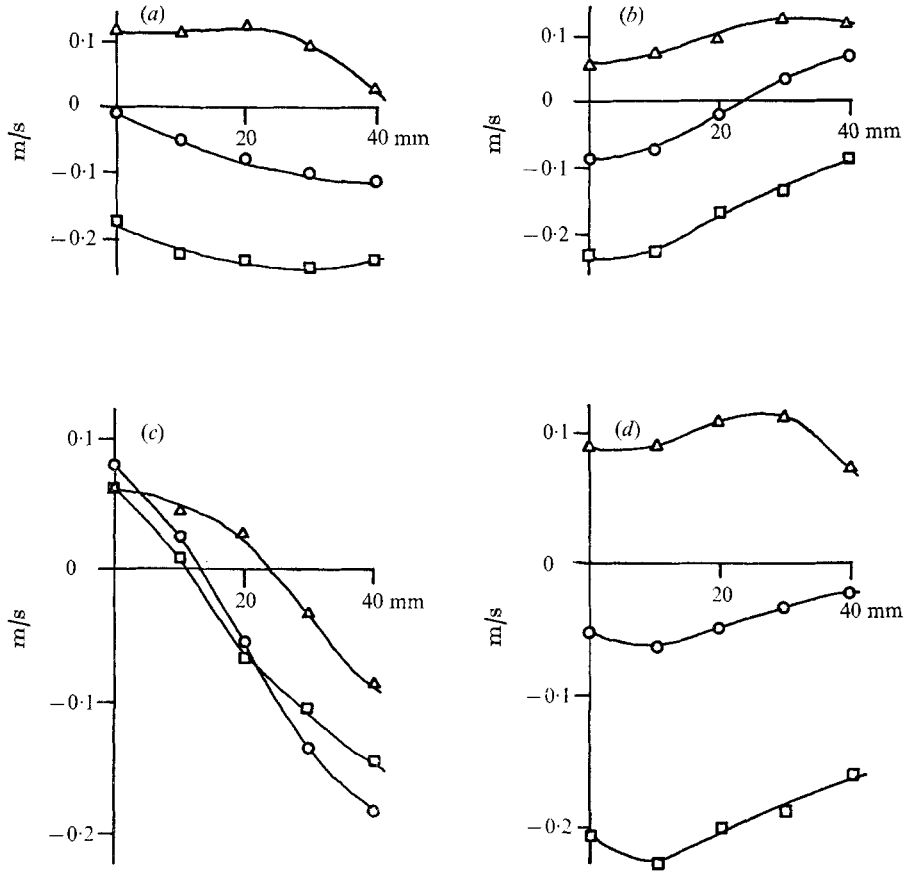

FIGURE 8. Spatial-advance technique. The horizontal axis gives the degree of spatial advance used. (*a*) Ordinary mean minus conditional mean for fronts; (*b*) ordinary mean minus conditional mean for backs; (c) conditional mean for backs minus conditional mean for fronts; (*d*) average of conditional means for fronts and backs. □, detector 25·4 mm, sensor 10·2 mm from wake centre; ○, detector 50·8 mm, sensor 35·6 mm from wake centre; △, detector 76·2 mm, sensor 61·0 mm from wake centre.

intermittency factor is much less critically dependent than the burst rate upon the precise adjustment of the turbulence detector.

The results of the present intermittency measurements differ somewhat from those reported by Townsend (1949*a*, *b*, 1956). If l_0 denotes half the distance between points on opposite sides of the wake at which the mean velocity defect is half its peak value, if y_0 is the distance between the wake centre-plane and the half-intermittency point and if σ_0 is the standard deviation of the profile of intermittency factor, then for the present flow

$$y_0/l_0 = 1{\cdot}7, \quad \sigma_0/y_0 = 0{\cdot}21,$$

whereas Townsend (1966) quotes $y_0/l_0 = 1{\cdot}8$ and $\sigma_0/y_0 = 0{\cdot}38$. The latter figure is confirmed by Gartshore (1966). It is difficult to understand the large discrepancy in σ_0/y_0, which according to the present measurements is close to the value found in a plane jet, but a partial explanation will be attempted in §5.1.

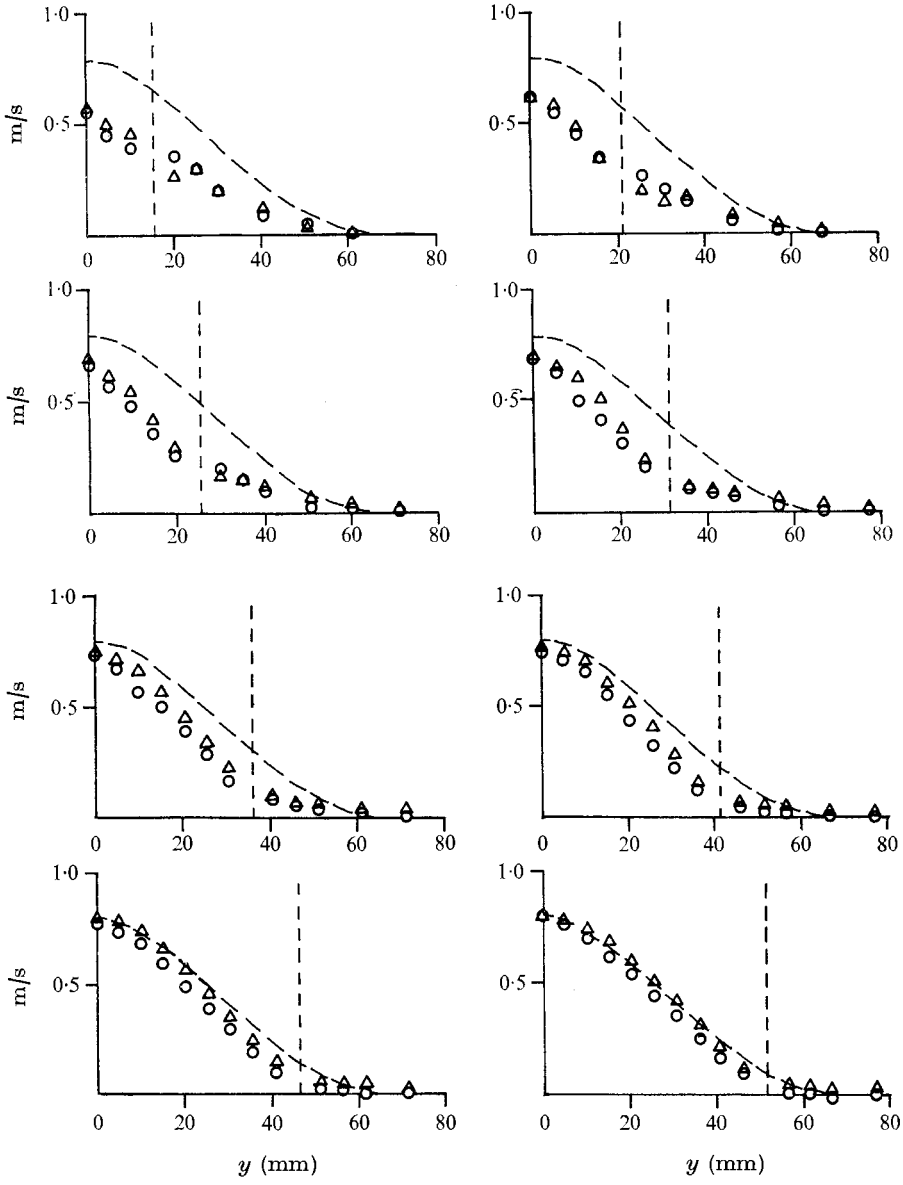

FIGURE 9. For legend see facing page.

3.4. *Conditional mean velocities*

The quantity actually measured was the difference between the conditional and ordinary mean velocities, the final result being obtained by adding the measured values to the ordinary profile in the course of the subsequent data reduction. It will be convenient to define, following Kovasznay *et al.* (1970), fronts as those instants at which the detector probe enters the turbulent zone and backs as the instants at which it leaves the turbulent zone. The hot wire which provides the signal sampled by the correlator will be called the sensor probe.

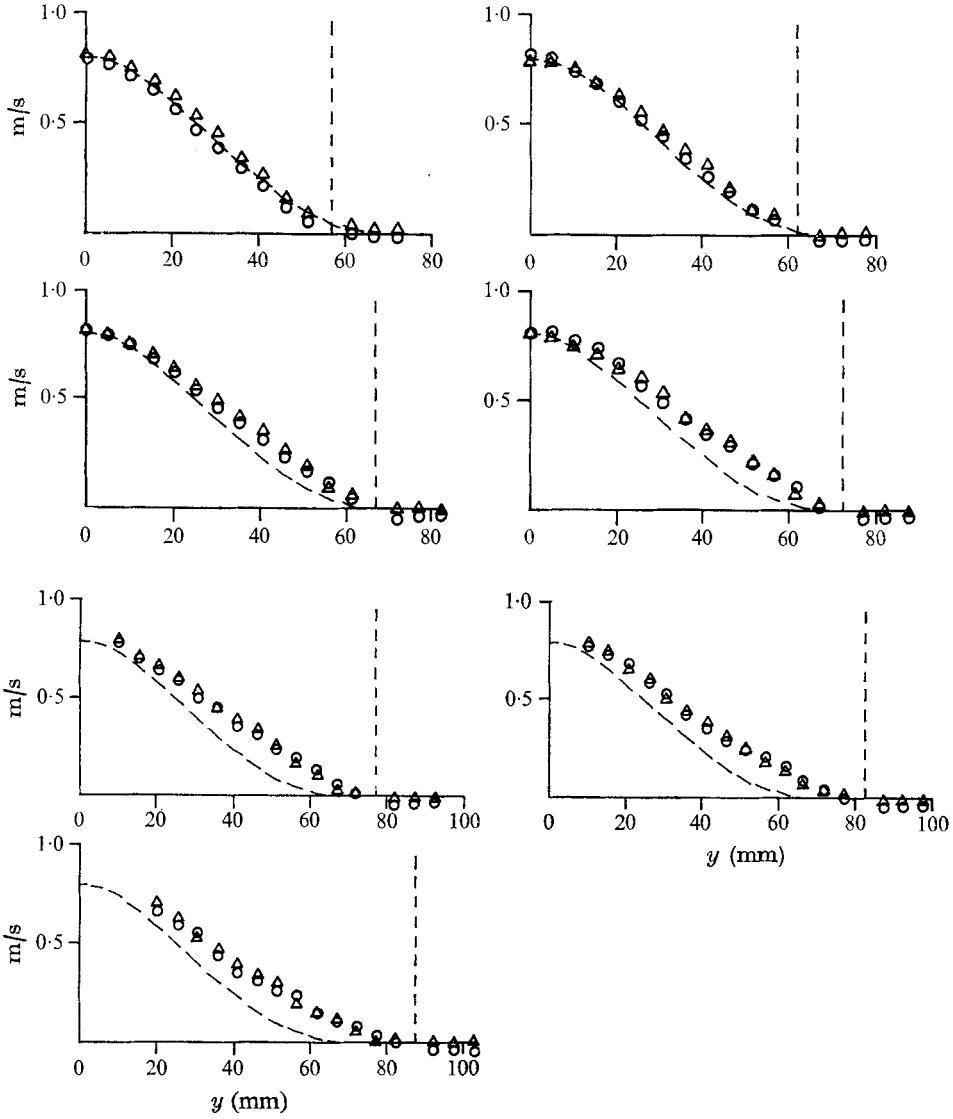

FIGURE 9. Conditional mean velocities. The horizontal axis gives the location of the sensor probe and the broken vertical line represents the position of the detector probe. — —, ordinary mean velocity profile; ○, samples taken on fronts; △, samples taken on backs.

The problem of the inherent delay in the turbulence detector requires careful attention before measurements of conditional mean velocity can be attempted. Inspection of oscillograms indicated a lag of about 2 ms, roughly the same for fronts and backs. To examine the validity of the spatial-advance technique explained in §2.3, a series of tests was carried out in which three typical conditional mean velocities were measured with differing degrees of detector advance. The results, shown in figure 8, indicated that spatial advance influences the measured conditional mean considerably. It had been hoped that the curves

would have a fairly simple structure which would suggest a suitable advance, but in fact unambiguous interpretation of the data is not possible. It was therefore necessary to rely on the oscillograms to determine the correct advance; the original estimate of 20 mm was firmly adopted and used for all subsequent measurements.

A set of conditional mean velocities is displayed in figure 9. Individual points were usually repeatable within 0·04 m/s, or 5 % of the peak velocity defect. Nearly all the uncertainty is due to the rather short averaging time available for each measurement, about three minutes. It is important to realize that the conditional means which are most difficult to measure are those which show a *large* deviation from the ordinary mean. This is because the larger deviations occur when the interface is in an unusual position, and so they are recorded by the sampling correlator not as a large meter reading but as a small reading which must then be multiplied by a large weighting factor. For example, the final graph in figure 9 corresponds to a case in which the turbulence boundary is in the required position only about twice per second (in contrast to a peak burst rate of 86 Hz), the results being weighted by a factor of nearly eight.

3.5. *Data from oscillograms*

In order to get more information about the structure of the turbulence boundary, the oscillograph was used to make two 6 s records of the intermittency signal at the half-intermittency point. The two traces were digitized and the data transferred to punched tape suitable for input to the digital computer. Mains voltage provided the time base for the traces, the nominal recording speed being 52 in./s. Each trace comprised about 500 bursts.

A computer program was written to calculate the autocorrelation of the intermittency signal. The random square wave $I(t)$ was stored in the form of about 500 pairs of numbers, each of which represented a front or back. The program formed the function $I(t)\,I(t+\tau)$ exactly and then averaged it, the process being repeated for a sequence of values of the parameter τ. The program also provided a print-out of the intermittency factor and burst rate of each sample. The intermittency factor was slightly below its nominal value of 0·5 in both cases.

The result of the computation displayed some unexpected features. Although the autocorrelation of each trace showed obvious periodicity, very similar to that reported by Townsend (1970), it was found that the positions of the maxima and minima were not the same for both traces. In fact, when the two separately computed autocorrelations are superposed, as shown in figure 10, the oscillations in the curves largely cancel out. It must be concluded that a sample of 500 bursts is insufficient to yield useful results. A more sensitive method involving longer averaging is necessary to confirm or disprove the presence of the periodic component in the turbulence boundary discussed by Grant (1958) and Townsend (1966, 1970). It would not be difficult to design a circuit to form $I(t+\tau)$ continuously from $I(t)$ and use a digital technique, similar to that employed in the probability analyser, to obtain the average of $I(t)\,I(t+\tau)$ over an arbitrarily long period, but the development of such

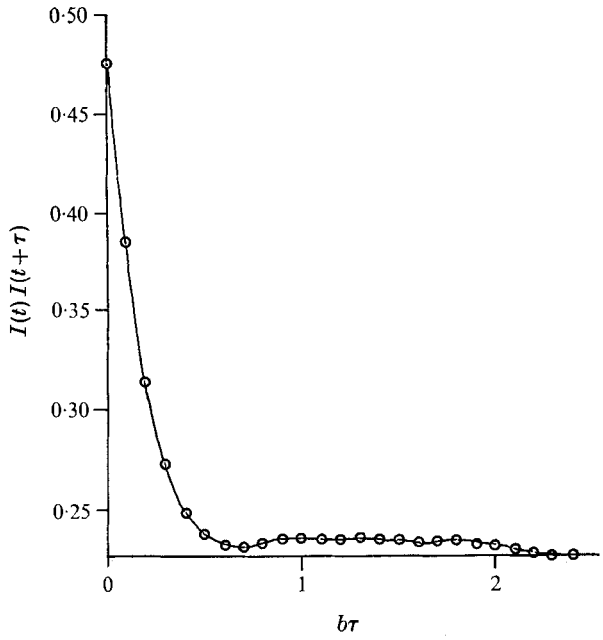

FIGURE 10. Autocorrelation of the intermittency signal. b = burst rate = 86 Hz. The sample intermittency factor is 0·476, so the autocorrelation approaches 0·227 as $\tau \to \infty$.

a system was not possible in the limited time available for the present experiments.

Another computer program scanned the traces to construct histograms representing the probability densities of the following quantities: the time between a front and the subsequent back; the time between a back and the subsequent front; the time between adjacent fronts; and the time between adjacent backs. These will be called, respectively, the *FB* density, the *BF* density, the *FF* density and the *BB* density. The results from the two traces showed no systematic differences and have been combined in figure 11, which also shows the curves corresponding to a Poisson model in which the probability of a front or back in time dt is supposed to be simply $2b\,dt$, where b is the burst rate. The applicability of this model will be discussed in §4.4.

The possibility of systematic errors in the histograms due to the effects of delays in the turbulence detector must be considered. The smoothing circuits incorporated to prevent spurious responses will effectively eliminate a burst of turbulence shorter than 2 ms within a long irritational stretch or an irrotational section of less than 2 ms in a long stretch of turbulence. Inspection of oscillograms indicates that perhaps 5–10 % of bursts are missed in this way, and also that short sections of irrotational flow are more often omitted than short turbulent bursts. The effect of such a turbulence detector is to weight unfairly the measured histograms in favour of larger intervals between the events considered, as pointed out by Corrsin & Kistler (1955). In the present measurements, the effects of detector faults are particularly noticeable in the *BF* density, but all the results are affected to some extent. In fact, the discrepancy between the histograms and the curves

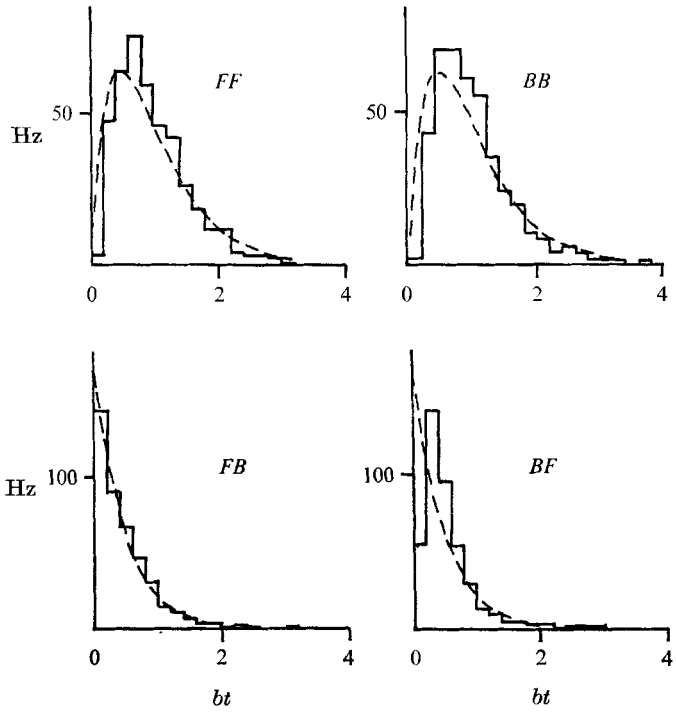

FIGURE 11. Probability densities from oscillograms.

predicted by the Poisson assumption may be due largely to experimental errors, although near the origin differences are to be expected for reasons to be pointed out in §4.4. The standard deviations (about the mean) of the histograms are

$$0{\cdot}45/b \quad \text{for} \quad FB, \quad 0{\cdot}58/b \quad \text{for} \quad FF,$$
$$0{\cdot}40/b \quad \text{for} \quad BF, \quad 0{\cdot}57/b \quad \text{for} \quad BB.$$

The Poisson values would be

$$1/2b \quad \text{for} \quad FB \text{ and } BF, \quad 1/b\sqrt{2} \quad \text{for} \quad FF \text{ and } BB.$$

3.6. *Measurements with the probability analyser*

The quantities analysed were u, the longitudinal component of the velocity fluctuation, and its time derivative $\partial u/\partial t$. Measurements were first made of the unconditional densities of u and $\partial u/\partial t$ at seven lateral positions in the wake. These are presented in figures 12 and 13. Since the measuring system is a.c. coupled, the first moments of the plotted densities are necessarily zero. Averaging times of about 40 s were used for these experiments.

A simple computer program was written to calculate the moments of the probability densities. The experimental points were effectively joined by straight-line segments and the moments evaluated by adding the contributions of the resulting elementary trapeziums. Each contributing term was also printed out explicitly

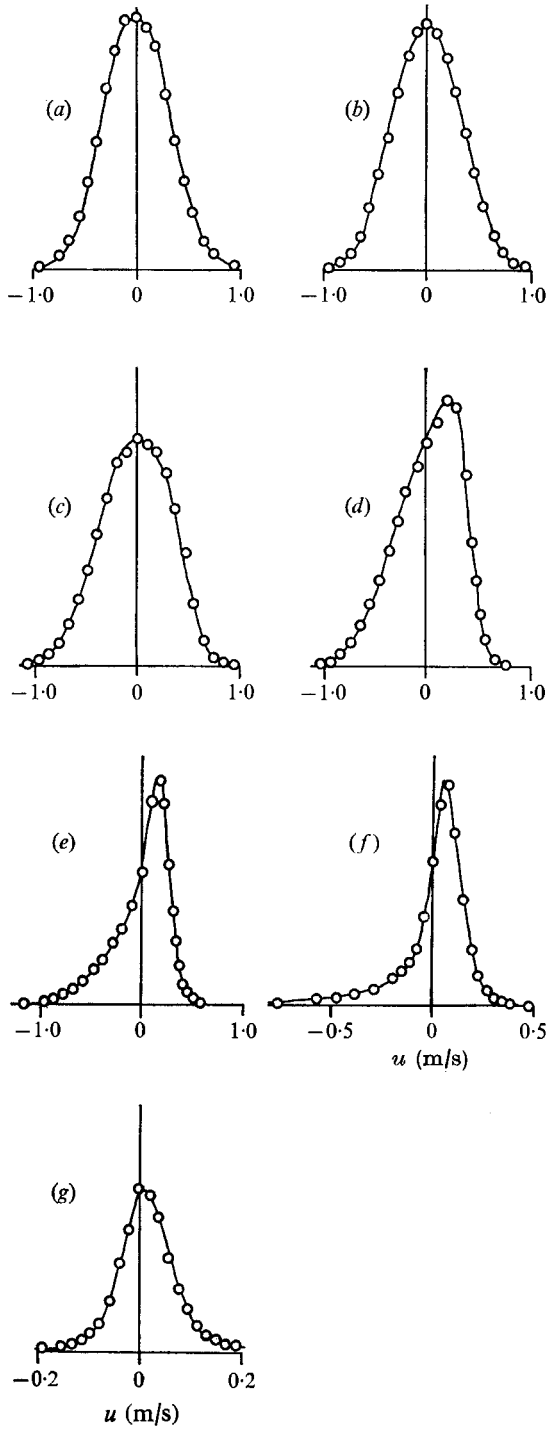

FIGURE 12. Unconditional probability density of u. (*a*) $y = 0$, (*b*) $y = 10{\cdot}2$ mm, (*c*) $y = 20{\cdot}4$ mm, (*d*) $y = 30{\cdot}5$ mm, (*e*) $y = 40{\cdot}6$ mm, (*f*) $y = 50{\cdot}8$ mm, (*g*) $y = 61{\cdot}0$ mm.

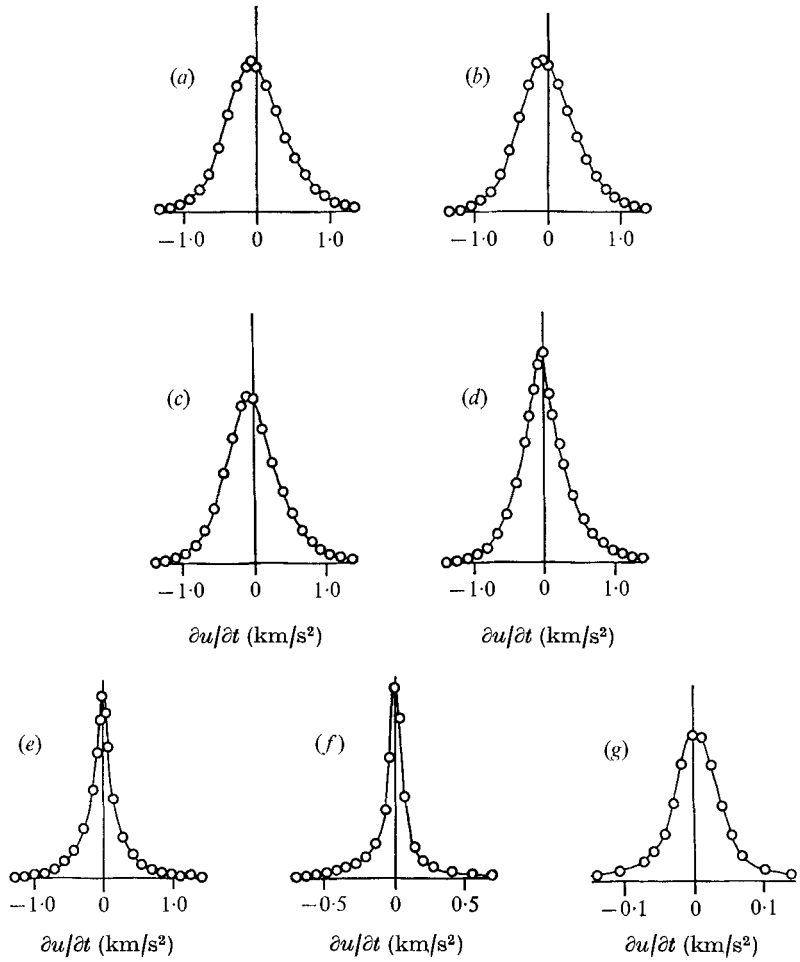

FIGURE 13. Unconditional probability density of $\partial u/\partial t$. (*a*) $y = 0$, (*b*) $y = 10{\cdot}2$ mm, (*c*) $y = 20{\cdot}4$ mm, (*d*) $y = 30{\cdot}5$ mm, (*e*) $y = 40{\cdot}6$ mm, (*f*) $y = 50{\cdot}8$ mm, (*g*) $y = 61{\cdot}0$ mm.

so that the reliability of the calculation could be assessed. Examination of typical contributions from the tails of the curves revealed large truncation errors in the calculated flatness and skewness factors, so these were discarded. The standard deviations, on the other hand, appeared to be quite accurate: the calculated $(\overline{u^2})^{\frac{1}{2}}$ was estimated to be less than 5 % low and $[\overline{(\partial u/\partial t)^2}]^{\frac{1}{2}}$ was probably less than 10 % low. These quantities are plotted in figures 14 and 15. There is a rather large discrepancy between the present values of $(\overline{u^2})^{\frac{1}{2}}$ and those reported by Townsend (1956, p. 140). Possible reasons for this will be discussed in §5.1.

Knowledge of $(\overline{u^2})^{\frac{1}{2}}$ and $[\overline{(\partial u/\partial t)^2}]^{\frac{1}{2}}$ permits calculation of the Kolmogoroff length scale if local isotropy is assumed. It was found to be about 0·3 mm at the station at which the present measurements were made. According to Corrsin & Kistler (1955), the thickness of the turbulence boundary is of the order of the Kolmogoroff microscale, so it follows that even with an ideal turbulence detector there is an uncertainty in the time of arrival of a front or back of at least 0·03 m/s.

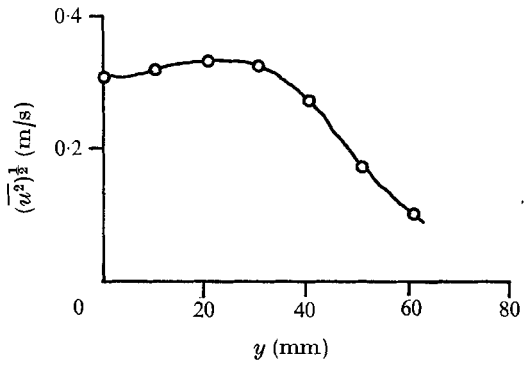

FIGURE 14. Profile of $(\overline{u^2})^{\frac{1}{2}}$.

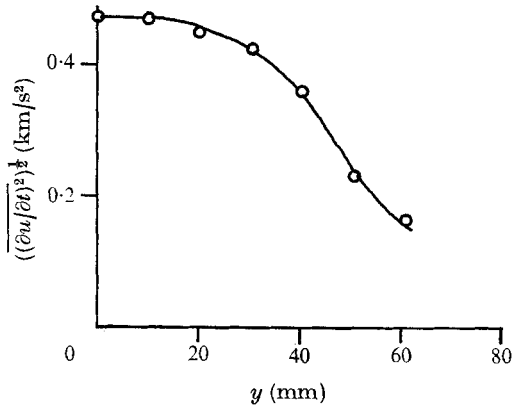

FIGURE 15. Profile of $[(\overline{\partial u/\partial t})^2]^{\frac{1}{2}}$.

By using the probability analyser in conjunction with the turbulence detector, probability densities in the turbulent and irrotational zones were separately measured at the half-intermittency point. To overcome the problem of lag in the turbulence detector a two-probe arrangement, similar to that employed for the conditional means, was used. Probe interference was avoided as follows. For the turbulent zone measurements the sensor probe was placed at 53·8 mm from the wake centre-plane, i.e. at the half-intermittency point, and the detector probe set up at 58·9 mm from the centre of the wake and 20 mm upstream. For the irrotational zone measurements the sensor probe was not moved, but the detector probe was repositioned at 48·7 mm from the wake centre, again 20 mm upstream. Now, if the flow is irrotational at 48·7 mm from the centre it is almost certainly irrotational at 53·8 mm, so the irrotational zone measurements are unlikely to be contaminated by turbulent bursts. A similar argument shows that the turbulent zone measurements are free from irrotational contributions.

The zone densities obtained by this technique are shown in figures 16 and 17. An interesting feature is the markedly non-Gaussian density of u within the turbulent zone, the departure from isotropic form possibly reflecting the influence of newly entrained fluid. Note that the origins of the graphs correspond to zero first moment of the unconditional densities. Computer calculations indicated that u in the turbulent zone was about 0·10 m/s lower than the ordinary mean while in the irrotational zone it was roughly 0·05 m/s higher. These two zone means should, in fact, be equal and opposite with respect to the ordinary mean (since the experiments were carried out at the half-intermittency point). This inconsistency, which could not be attributed to truncation errors in the numerical evaluation of the means, is probably a consequence of the probe arrangement described above. It seems unlikely, however, that the general shape of the curves is seriously incorrect.

The series of measurements using the probability analyser was completed by an experimental test of part of the well-known theory of Phillips (1955): that the r.m.s. longitudinal fluctuation intensity in the irrotational zone falls off inversely as the square of the distance from the wake centre-plane. Since the

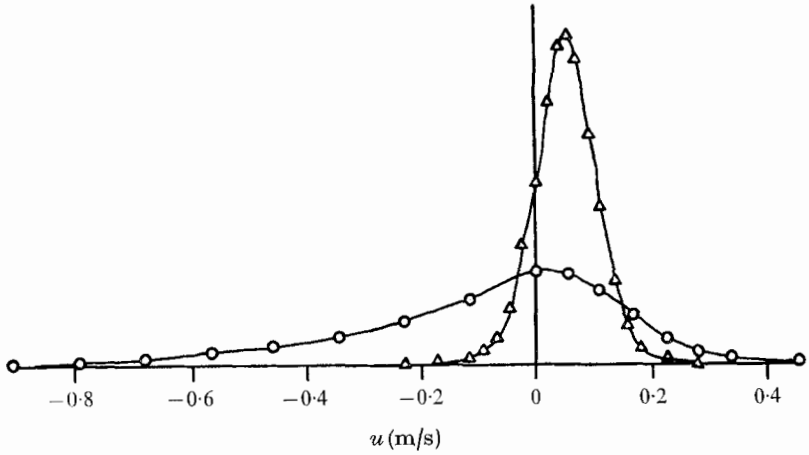

FIGURE 16. Zone probability density of u. ○, turbulent zone; △, irrotational zone.

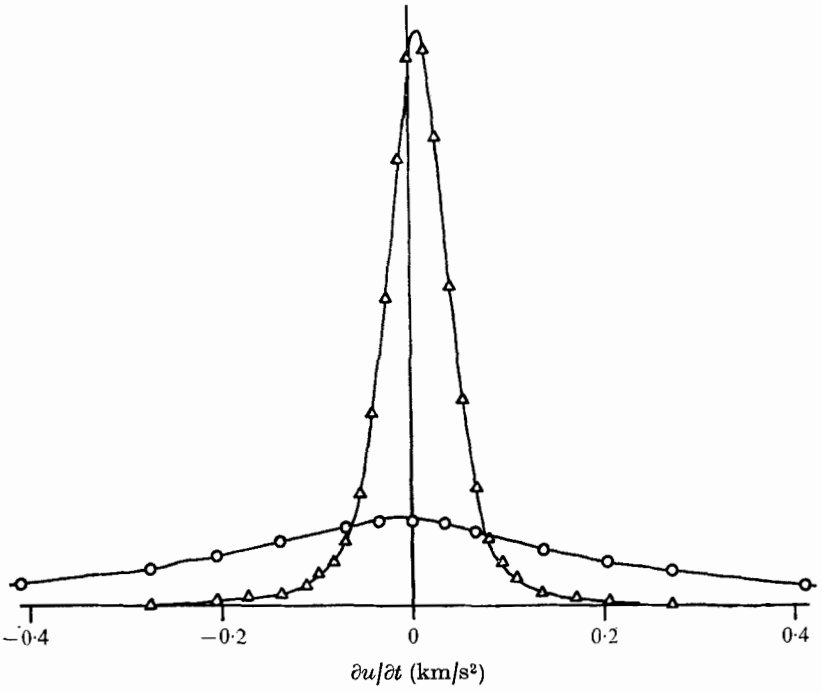

FIGURE 17. Zone probability density of $\partial u/\partial t$. ○, turbulent zone; △, irrotational zone.

probability density of u in the irrotational zone was found to be approximately Gaussian at the half-intermittency point and may reasonably be expected to be so further out, it is possible to estimate the variation of the fluctuation intensity by observing the peak of the probability density at a series of positions near the wake edge. The analyser was therefore set up to measure irrotational zone densities, using the spatial-advance technique in the intermittent region and

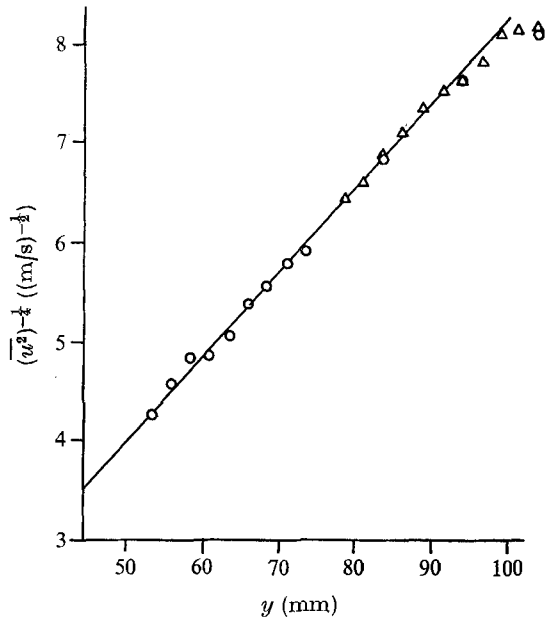

FIGURE 18. Comparison with Phillips's (1955) theory. ○, using spatial-advance technique; △, using single probe.

simply a single probe well outside the wake, and the peak density at various positions found by trial and error. The data are displayed in figure 18. Except at distances from the centre-plane greater than about 95 mm, where the effect of the boundary layer on the roof of the tunnel becomes appreciable, the results are in agreement with the theoretical prediction. Furthermore, the experimental points are fitted by a straight line right up to the half-intermittency point, although Phillips' theory is strictly applicable only at large distances from the wake centre. A similar effect has been reported by Kovasznay *et al.* (1970) and Wygnanski & Fiedler (1970).

4. Some formal relationships

4.1. *Interface slope*

The intermittency function is defined as

$$I(\mathbf{r},t) = \begin{cases} 1 & \text{if flow at } \mathbf{r} \text{ is turbulent,} \\ 0 & \text{otherwise.} \end{cases}$$

In the course of the present experiments y was the only component of the position vector $\mathbf{r}$ to be varied (ignoring the complications of the spatial-advance technique), so the dependence on x and z will be suppressed and the intermittency function will be written as $I = I(y,t)$. It is an immediate consequence of the definition that

$$I(y,t) - I(y+dy,t) = \begin{cases} 1 & \text{if } y < h < y+dy, \\ 0 & \text{otherwise,} \end{cases} \tag{1}$$

where $h(t)$ is the instantaneous interface location. It will be assumed throughout that the interface is not folded over onto itself, i.e. that $h(t)$ is single-valued. Averaging (1) over time yields the probability density for interface position:

$$f(y) = -\bar{I}'(y), \tag{2}$$

where $\bar{I}' = d\bar{I}/dy$; this is a well-defined quantity although $I(y,t)$ is not itself everywhere differentiable.

The experimental results indicate that the burst rate $b(y)$ and the probability density $f(y)$ are Gaussian and that they have the same standard deviation, so

$$b(y) = Kf(y), \tag{3}$$

where K is a constant. Now let $F(p,q)$ denote the joint probability density for h and $|\dot{h}|$, so that $F(p,q)\,dp\,dq$ is the probability that $p < h < p+dp$ and simultaneously $q < |\dot{h}| < q+dq$. Then consider

$$[I(y,t) - I(y+dy,t)]\,|\dot{h}|$$

as a function of time. If dy is very small, the function consists of a train of pulses, the area enclosed by each being dy. The average number of pulses per unit time is $2b(y)$, hence

$$\overline{[I(y,t) - I(y+dy,t)]|\dot{h}|} = 2b(y)\,dy, \tag{4}$$

or equivalently, in virtue of the definition of $F(p,q)$,

$$\int_0^\infty F(p,q)\,q\,dq = 2b(p) = 2Kf(p), \tag{5}$$

assuming the validity of (3). It follows immediately that

$$\overline{|\dot{h}|} = \int_0^\infty \int_{-\infty}^\infty F(p,q)\,q\,dp\,dq = 2K\int_{-\infty}^\infty f(p)\,dp = 2K \tag{6}$$

and

$$\overline{h|\dot{h}|} = \int_0^\infty \int_{-\infty}^\infty F(p,q)\,pq\,dp\,dq = 2K\int_{-\infty}^\infty pf(p)\,dp = \overline{|\dot{h}|}\,\bar{h}.$$

In other words, the experimental result that $b(y)$ and $f(y)$ have the same shape implies that the modulus of the slope of the interface is uncorrelated with its position. It does not necessarily follow that h and $\dot{h}$ are uncorrelated.

Assuming that the turbulence boundary is convected at 10 m/s, equation (6) yields $\overline{|dh/dx|} = 0{\cdot}48$ for the present case; this lends some support to the assumption of a single-valued $h(t)$. If $f(y)$ and $b(y)$ are not simply related by (3), then a more general result may be obtained from (5):

$$\overline{|\dot{h}|} = 2\int_{-\infty}^\infty b(p)\,dp. \tag{7}$$

It may also be shown that $I(y,t)$ and $|\dot{h}(t)|$ are uncorrelated. Equation (4) may be written in the form

$$-d\overline{(I(y,t)\,|\dot{h}|)}/dy = 2b(y),$$

so that

$$\overline{I(y,t)\,|\dot{h}|} = 2\int_y^\infty b(p)\,dp = 2K\int_y^\infty f(p)\,dp = \overline{|\dot{h}|}\,\bar{I}(y).$$

Use has been made of (3), (6) and (2), with the convention $I(\infty,t) = 0$ for all t.

4.2. *Conditional sampling*

Consider an experiment designed to measure conditional mean velocities by sampling the anemometer signal for an effectively infinitesimal interval each time a pulse of the appropriate sign arrives from the turbulence detector. This is the method used by Kovasznay *et al.* (1970) and Wygnanski & Fiedler (1970). Let

$$t_1^F, t_2^F, t_3^F, \ldots,$$
$$t_1^B, t_2^B, t_3^B, \ldots,$$

be the sampling instants for fronts and backs respectively. Then the measured conditional means are simply

$$\left.\begin{aligned} X^F(y,\eta) &= \lim_{N\to\infty} \frac{1}{N} \sum_{i=1}^{N} u(y, t_i^F(\eta)), \\ X^B(y,\eta) &= \lim_{N\to\infty} \frac{1}{N} \sum_{i=1}^{N} u(y, t_i^B(\eta)), \end{aligned}\right\} \tag{8}$$

where η is the position of the interface (or of the detector probe), y is the position at which the velocity is sensed and $u(y,t)$ is now the total longitudinal fluid velocity. For the sake of clarity the following argument will be expressed in terms of equipment set up to receive fronts (rather than backs), but the superscript F will be dropped. The case of a sampling correlator acting only on backs is, of course, formally identical. Define

$$Q(\tau, d\tau, t) = \begin{cases} 1 & \text{if } \tau < \text{time since last front} < \tau + d\tau, \\ 0 & \text{otherwise.} \end{cases}$$

Then consider the quantity

$$L(y,\eta,\tau) = \lim_{d\tau\to 0} \lim_{N\to\infty} \frac{\sum_{i=1}^{N} Q(\tau, d\tau, t_i)\, u(y,t_i)}{\sum_{i=1}^{N} Q(\tau, d\tau, t_i)}.$$

This is a kind of conditional mean which could in principle be measured by taking samples only when the interface is in the specified position and simultaneously the time since the last front is in the correct small range. Let $\phi(\tau)$ be the probability density for the time interval between successive fronts (i.e. the FF density discussed in § 3.5 and displayed in figure 11). It is easily seen that

$$X(y,\eta) = \int_0^\infty L(y,\eta,\tau)\, \phi(\tau)\, d\tau. \tag{9}$$

Now recall the method of sampling used for the present experiments. At the instant at which the interface is in the specified position the velocity signal is sampled and then held for 92 ms, during which the correlator ignores further fronts; at the end of the hold period the gates are promptly reset. Since the correlation time of the intermittency signal is much less than 92 ms, the action of the sampler can be modelled by supposing that it begins to operate at a random instant, independent of the state of the intermittency signal, and then takes a sample at the instant of arrival of the first subsequent front. As will be shown below, this model implies that the probability of the instant of operation lying

between two fronts whose separation is in a range $d\tau$ at τ is $b(\eta)\,\tau\phi(\tau)\,d\tau$, where $b(\eta)$ is the burst rate at the location of the detector probe. Hence the present conditional mean velocities can be expressed in the form

$$U(y,\eta) = b(\eta)\int_0^\infty L(y,\eta,\tau)\,\tau\phi(\tau)\,d\tau. \tag{10}$$

Inspection of (9) and (10) shows that $X(y,\eta)$ and $U(y,\eta)$ are, in general, different. An obvious sufficient condition for the identity of $X(y,\eta)$ and $U(y,\eta)$ is that $L(y,\eta,\tau)$ should be independent of τ, but the physical implications of such an assumption are unclear. Nevertheless, it seems likely that a turbulence detector considerably more efficient than that described here would be needed to distinguish between the two types of conditional mean.

Two useful integral relations will now be derived. It is possible to express the conditional mean velocity in a way different from, but equivalent to, the formulation (8). Thus

$$X^F(y,\eta)+X^B(y,\eta) = \lim_{d\eta\to 0}\overline{\frac{|\dot{h}(t)|}{b(\eta)\,d\eta}\,[I(\eta,t)-I(\eta+d\eta,t)]\,u(y,t)}.$$

The factor $|\dot{h}|/b(\eta)\,d\eta$ arises from the necessity of giving equal weight to each velocity sample. Rearrangement and integration with respect to η yields

$$\begin{aligned}\int_\eta^\infty [X^F(y,\xi)+X^B(y,\xi)]\,b(\xi)\,d\xi &= \lim_{d\eta\to 0}\overline{\frac{|\dot{h}|u(y,t)}{d\eta}\int_\eta^\infty [I(\xi,t)-I(\xi+d\eta,t)]\,d\xi}\\ &= \overline{|\dot{h}|\,u(y,t)\,I(\eta,t)},\end{aligned}$$

where use has been made of the almost obvious fact that

$$\lim_{d\eta\to 0}\frac{1}{d\eta}\int_\eta^\infty [I(\xi,t)-I(\xi+d\eta,t)]\,d\xi = I(\eta,t)$$

for all η and t. The result that $I(\eta,t)$ and $|\dot{h}|$ are uncorrelated suggests the assumption that $I(\eta,t)\,u(y,t)$ and $|\dot{h}|$ are uncorrelated, although there is no experimental evidence for this. Hence

$$\frac{1}{B}\int_\eta^\infty X^{FB}(y,\xi)\,b(\xi)\,d\xi = \overline{u(y,t)\,I(\eta,t)}, \tag{11}$$

where

$$X^{FB}(y,\xi) = \tfrac{1}{2}[X^F(y,\xi)+X^B(y,\xi)],$$

$$B = \int_0^\infty b(p)\,dp$$

and use has been made of (7). Setting $y=\eta$ in (11) yields

$$\frac{1}{B}\int_y^\infty X^{FB}(y,\xi)\,b(\xi)\,d\xi = \overline{u(y,t)\,I(y,t)}.$$

The right-hand side is the turbulent zone mean velocity at y. Setting $\eta = 0$ in (11) and taking $I(0,t) = 1$ for all t,

$$\frac{1}{B}\int_0^\infty X^{FB}(y,\xi)\,b(\xi)\,d\xi = \overline{u(y,t)}, \tag{12}$$

where the right-hand side is now the ordinary mean velocity at y.

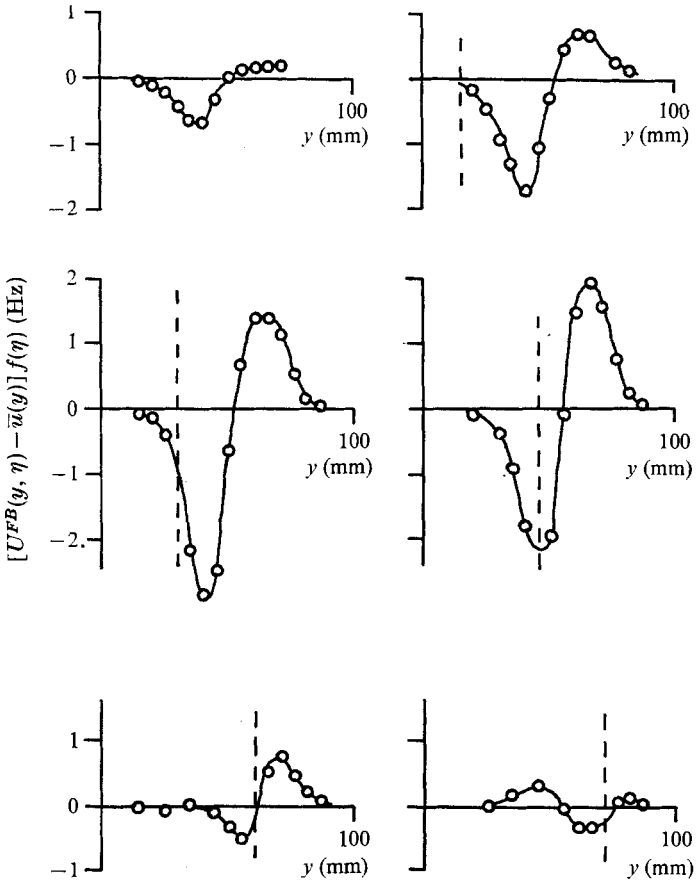

FIGURE 19. Illustrating equation (12). The horizontal axis gives η and the broken vertical line represents the value of the parameter y (which is zero in the first graph).

To examine the applicability of these formulae, the experimental data have been used to plot the quantity

$$[U^{FB}(y,\eta)-\bar{u}(y)]f(\eta)$$

as a function of η for various values of the parameter y. Here $U^{FB} = \frac{1}{2}(U^F + U^B)$ is the conditional mean obtained by the sample-and-hold method. Typical results are shown in figure 19. According to (12) the area beneath each curve should be zero if $X^{FB}(y,\eta)$ and $U^{FB}(y,\eta)$ are regarded as equivalent and if equation (3) is assumed to be valid. In view of the several possibly unjustified approximations which must be made in order to arrive at the simple form (12), the lack of precise agreement is not surprising.

4.3. *Profile of the FF and BB densities*

The model of the sampling correlator as a device activated at a random instant has been explained above. An expression will now be derived giving the average time the sampler has to wait before encountering a front. Let $\phi(\tau)$ be the probability density for the time between fronts, as before. Then in a long period T

the fraction of intervals between successive fronts which lie in a range $d\tau$ at τ is $\phi(\tau)\,d\tau$, so the proportion of the period T covered by intervals of this class is $b\tau\phi(\tau)\,d\tau$, where b is the average number of fronts per unit time, i.e. the burst rate. Since the model requires the instant of operation to be random, this is also the probability of the reset moment finding itself in an interval between fronts in the range $d\tau$ at τ. This result has already been used in § 4·2. Given that the reset moment is, in fact, in such an interval, it is clear that the probability of the subsequent front occurring before time s has elapsed is

$$\begin{cases} s/\tau & \text{for} \quad s < \tau, \\ 1 & \text{for} \quad s > \tau. \end{cases}$$

Hence the chance of a front before time s has elapsed, now regardless of the class in which the reset moment finds itself, is

$$\alpha(s) = b\int_0^s \tau\phi(\tau)\,d\tau + bs\int_s^\infty \phi(\tau)\,d\tau.$$

Notice that $\alpha(0) = 0$ and $\alpha(\infty) = 1$ (as required) in virtue of the identities

$$\int_0^\infty \phi(\tau)\,d\tau = 1, \quad b\int_0^\infty \tau\phi(\tau)\,d\tau = 1.$$

Differentiation yields the probability density for the waiting time:

$$\alpha' = \frac{d\alpha}{ds} = b\int_s^\infty \phi(\tau)\,d\tau,$$

and the mean waiting time can be calculated directly:

$$\bar{s} = \int_0^\infty s\alpha'(s)\,ds = b\int_0^\infty s\left[\int_s^\infty \phi(\tau)\,d\tau\right]ds$$

$$= b\int_0^\infty \phi(\tau)\left[\int_0^\tau s\,ds\right]d\tau = \tfrac{1}{2}b\int_0^\infty \phi(\tau)\tau^2\,d\tau.$$

The change in the order of integration is clearly permissible in view of the form of $\phi(\tau)$. The result can also be expressed in terms of the variance ϵ of $\phi(\tau)$:

$$\bar{s} = (1+\epsilon^2 b^2)/2b. \tag{13}$$

The weighting factor, defined in § 2.4 and denoted here by $W(y)$, is related to the average waiting time by

$$\bar{s} = H(W-1), \tag{14}$$

where H is the hold time, 92 ms in the present case. Equations (13) and (14) together yield

$$\epsilon(y) = [2bH(W-1)-1]^{\frac{1}{2}}/b, \tag{15}$$

which permits the profile of the second moment of the FF and BB densities to be calculated from the measurements of weighting factor. Reduction of the experimental data leads to the plot shown in figure 20. As might be expected, the scatter is rather large, but there is quite good agreement with the standard deviation of $\phi(\tau)$ found directly from the histograms of figure 11. From (15)

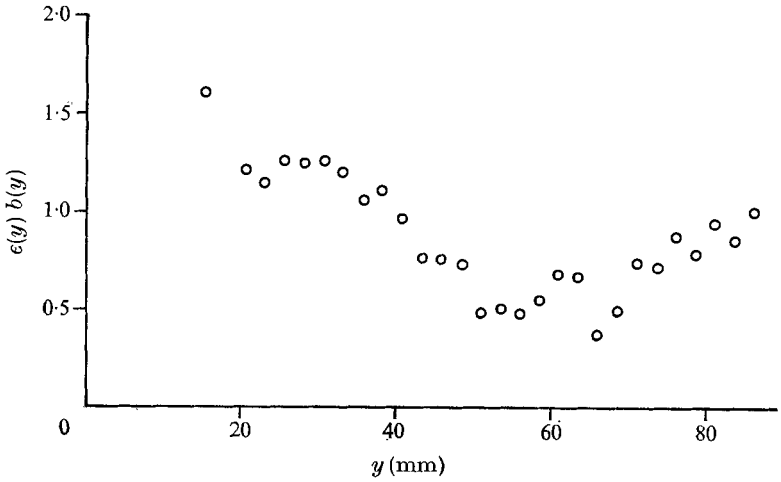

FIGURE 20. Illustrating equation (15).

it can be estimated that at the half-intermittency point $\epsilon b = 0{\cdot}6 \pm 0{\cdot}1$, whereas the results of §3.5 indicate $\epsilon b = 0{\cdot}58$. If $\phi(\tau)$ is assumed to be Poisson, then $\epsilon b = 1/\sqrt{2}$, showing no dependence on position. In fact, it is possible that the apparent variation of ϵb across the wake is due largely to imperfections in the turbulence detector.

4.4. *Application of noise theory*

Since the probability density for interface position is known to be approximately Gaussian, it is natural to try to adapt the results of the well-developed theory of normally distributed noise in order to explain some of the statistical properties of the interface. Most of the required material is contained in the comprehensive papers of Rice (1944, 1945). The applicability of noise theory to the problem of the turbulence boundary has been previously pointed out by Corrsin & Kistler (1955) and more recently by Kovasznay *et al.* (1970).

Define

$$a(t) = h(t) - \bar{h}$$

and denote its autocorrelation by

$$R(\tau) = \overline{a(t)\, a(t+\tau)}. \tag{16}$$

Then $a(t)$ is to be regarded as a normally distributed noise signal with zero mean. It follows that $\dot{a}(t)$ is also normally distributed and is independent of $a(t)$. It is also easily proved that

$$R''(0) = -\overline{\dot{a}^2}, \tag{17}$$

where R'' denotes $d^2R/d\tau^2$. Rice has shown that

$$b_0 = \frac{1}{2\pi}\left[-\frac{R''(0)}{R(0)}\right]^{\frac{1}{2}}, \tag{18}$$

where b_0 is half the number of zero crossings of $a(t)$ per unit time, corresponding in the present case to the burst rate at the half-intermittency point. Equations

(16), (17) and (18) together, used in conjunction with the Taylor hypothesis, permit an estimate of the r.m.s. slope of the interface. The r.m.s. slope can also be derived directly from (6) since $(\overline{\dot{a}^2})^{\frac{1}{2}} = (\frac{1}{2}\pi)^{\frac{1}{2}}\overline{|\dot{a}|}$ if $\dot{a}(t)$ is normally distributed. Another formula quoted by Rice may be stated in the present notation as

$$b(y) = b_0 \exp[-(y-\bar{h})^2/2R(0)].$$

Hence, as might be expected, the noise model implies a Gaussian burst rate with the same standard deviation as the intermittency factor and peaking at the half-intermittency point. An interesting formula relates $R(\tau)$ to the autocorrelation of the intermittency function, which is experimentally available:

$$S(\tau) = \frac{2}{\pi}\sin^{-1}\left[\frac{R(\tau)}{R(0)}\right],$$

where $S(\tau)$ is the autocorrelation of the function $2I(\bar{h}, t) - 1$. It must be emphasized that the validity of this result depends upon the assumption that the interface has normal statistics. The errors in the experimental autocorrelation unfortunately preclude the evaluation of $R(\tau)$ through these formulae.

Rice was unable to solve completely the problem which in the present context corresponds to prediction of the FB and BF densities. These are, of course, identical for the noise model considered here, and will be denoted by $\psi(\tau)$. Rice's analysis yields only the probability of a back in the interval $d\tau$ at τ given that there has been a front at $\tau = 0$, regardless of any intervening fronts and backs. There does not seem to be a simple relationship between this probability and the required $\psi(\tau)$ except in the limits $\tau \to 0$ and $\tau \to \infty$. If τ is chosen so small that there is negligible chance of more than one back within it,

$$\psi(\tau) \to \frac{\tau}{8}\left(\frac{R(0)\,R^{(4)}(0) - [R''(0)]^2}{-R(0)\,R''(0)}\right) \quad \text{as} \quad \tau \to 0.$$

Corrsin & Kistler (1955) have given a physical argument for the linear behaviour of $\psi(\tau)$ near the origin. On the other hand, if τ is much larger than the correlation time of $a(\tau)$, the probability of a back in the interval $d\tau$ at τ becomes independent of the presence of a front at $\tau = 0$ and tends to the constant value $b_0 d\tau$, leading to the result

$$\psi(\tau) \to 2b_0 e^{-2b_0\tau} \quad \text{as} \quad \tau \to \infty.$$

If the times of arrival of fronts and backs satisfied Poisson statistics the FB and FF densities would be respectively

$$\psi(\tau) = 2b_0 e^{-2b_0\tau}, \quad \phi(\tau) = 4b_0^2 \tau e^{-2b_0\tau}.$$

Hence the use of these forms to fit the histograms of figure 11 is consistent with the noise model only in the limit $\tau \to \infty$. At small τ the Poisson model fails, since it is based on the assumption, clearly untenable on physical grounds, that the probability of a front in an infinitesimal time interval is independent of the presence of a front in an arbitrarily closely neighbouring interval.

5. Discussion and conclusions

5.1. *Comparison with earlier experiments*

Intermittency factors have been measured by Townsend (1948, 1949*a*, *b*) in the plane wake; by Corrsin & Kistler (1955) in the boundary layer and axisymmetric jet; by Klebanoff (1955) in the boundary layer; by Bradbury (1965) and Heskestad (1965) in the plane jet; by Fiedler & Head (1966) in a boundary layer; by Schapker (1966) in an axisymmetric wake; by Gartshore (1966, 1967) in plane wall jets and wakes in tailored pressure gradients; by Snyder & Margolis (1967) in the curved mixing layer; by Demetriades (1968) and Wygnanski & Fiedler (1969) in the axisymmetric wake and jet, respectively; by Mobbs (1968) in the zero-defect wake; by Kovasznay *et al.* (1970) in the boundary layer; and by Wygnanski & Fiedler (1970) in the plane mixing layer. The results are similar in all cases and show that the profile of intermittency factor is well represented by the error function, implying a Gaussian probability density for interface position. Measurements of burst rate are less numerous, but the published data seems to support the view, clearly suggested by the present experiments, that the burst-rate and intermittency curves have the same standard deviation. The boundary-layer measurements of Kovasznay *et al.* (1970) indicate that the standard deviations are equal within 5 %. Results in a plane mixing layer obtained by Wygnanski & Fiedler (1970) seem to show that the standard deviation of the burst rate is rather higher than that of the intermittency factor, but this disagreement is probably due to the difficulty in interpreting the results which arises from the fact that the intermittency factor is less than unity throughout the flow. These observations suggest that it is a characteristic of plane flows that the modulus of the slope of the turbulence boundary is independent of its position.

There is a discrepancy between the present intermittency measurements and those of Townsend, who obtained self-consistent results using both a turbulence detector and a method based on measurement of the flatness factor of velocity derivatives at various points across the flow. An examination of the hypotheses underlying the flatness-factor technique (Townsend 1956, p. 145) indicates that errors will be incurred if the turbulent zone is inhomogeneous, or if fluctuations of the velocity derivatives are appreciable in the irrotational zone. Figure 17 reveals the presence of both these effects, and although a simple calculation shows that the errors produced by the two causes are in opposite directions, the data of Wygnanski & Fiedler (1970) suggest that the overall result is that the apparent intermittency factor obtained by the flatness-factor method is low. Close examination of Townsend's (1949*a*) results suggests that the disagreement with the present experiments may also be simply attributable to the difficulty in interpreting rather scattered data. The differences between the turbulence-detector measurements may be due to the different procedures used to set up the circuits.

Conditional mean velocities have been previously measured by Kovasznay *et al.* (1970) and Wygnanski & Fiedler (1970). The present experiments agree with these studies in showing that the instantaneous interface position is closely correlated with the flow distribution over a large proportion of the wake. When

the turbulent zone is wider than usual there is (in the case of the wake) a general retardation of turbulent fluid, whereas a contracted turbulent zone is associated with downstream velocities greater than the average. The present measurements are more closely in agreement with those of Wygnanski & Fiedler in that there appears to be a discontinuity in the gradient of the conditional mean velocity at the interface. The slope within the turbulent zone, although roughly constant for a given interface position, varies with the position of the interface. The data of Kovasznay *et al.* show a practically constant slope in the turbulent zone and no noticeable discontinuity at the turbulence boundary. It is not clear whether these differences are real or merely reflect instrumental imperfections. In none of the flows investigated is there evidence of a discontinuity at the interface of the conditional mean velocity itself, as has been supposed by Townsend (1966, 1970), nor of an inflexion of the type described by Betchov & Criminale (1964). The linear form of the conditional mean has been predicted by Nee & Kovasznay (1969).

The longitudinal conditional mean velocities measured by Kovasznay *et al.* and Wygnanski & Fiedler did not reveal any differences between samples taken on fronts and samples taken on backs, whereas small but definite differences are apparent in the present results. Of course, there is no reason why sampling on fronts and backs should give the same mean, but it is thought that the present differences cannot be regarded as significant. In figure 8 it was shown that differences between the fronts and backs measurements were rather critically dependent upon the degree of spatial advance used, while the average of the two is less sensitive. It would therefore be unwise to expect the spatial-advance technique to resolve accurately the difference between samples taken on fronts and backs, although the average of the two types of mean may be substantially correct. The delay-line technique described by Kovasznay *et al.* appears to be the only satisfactory solution to these problems.

The probability densities of the longitudinal velocity component and its derivation are in general agreement with the measurements of Townsend (1947, 1948) and Klebanoff (1955). They are not inconsistent with the view that the turbulence in the core of the wake may be regarded as isotropic. The zone densities, which have a shape similar to that found by Snyder & Margolis (1967) in a curved mixing layer, have already been discussed above.

Although the results of the present measurements in the irrotational zone are in agreement with the theory of Phillips (1955), the origin of the straight line fitting the data is nearly at the wake centre, whereas the data obtained by Townsend and quoted by Phillips (1955), together with the later experiments of Bradbury (1965) and Bradshaw (1967) in other flows, suggest that the virtual origin lies at a point where the intermittency factor is between 0·8 and 0·9. These earlier experiments were carried out without the aid of a turbulence detector, and although confined to regions of low intermittency they were nevertheless susceptible to contamination by tongues of turbulence, the effect of which would be to move the virtual origin away from the centre of the wake. The genuinely irrotational-zone measurements of Kovasznay *et al.* (1970) and Wygnanski & Fiedler (1970) are in much better agreement with the present results.

The histograms representing the FB and BF densities may be compared with

those in a boundary layer reported by Corrsin & Kistler (1955). The agreement is not good near the origin, owing to differences between designs of the turbulence detectors, but their results do not appear to differ significantly from those presented here. Corrsin & Kistler did not measure the FF and BB densities, but have given the FB and BF densities at points other than the half-intermittency point.

Corrsin & Kistler (1955) and Kovasznay *et al.* (1970) have shown that in the boundary layer the spectrum of the intermittency signal has the simple form associated with a random square wave with Poisson-distributed jump instants. Such a spectrum implies an exponential autocorrelation. Although the present data are not inconsistent with these results, it should be remembered that the Poisson model is not strictly applicable, as explained in §4.4. Owing to the uncertainties arising from the inadequate length of the oscillograms it cannot be conclusively stated that there is no (weak) periodic component in the intermittency signal. Indeed, Demetriades (1968) has found periodic structure in the turbulence boundary in an axisymmetric wake and Grant (1958) has reported the occurrence of groups of equally spaced contortions of the interface in a plane wake.

The longitudinal r.m.s. turbulence intensity presented here is about 33 % higher than that reported by Townsend (1956, p. 140). Several possible explanations were initially considered: (i) wire-length effect or a peculiarity in the design of the anemometers may result in differences between the static and dynamic sensitivities (Corrsin 1963; Champagne, Sleicher & Wehrmann 1967); (ii) the static calibration procedure may itself be incorrect (Collis & Williams 1959; Bruun 1971; Perry & Morrison 1971); (iii) probe vibration may cause an apparently high turbulence intensity; (iv) the present anemometers may have a much larger bandwidth than Townsend's constant-current system; (v) at a given number of diameters downstream, the ratio of r.m.s. intensity to free-stream speed may be dependent on Reynolds number; (vi) the present flow may not be typical of a plane wake owing to gross disturbance by the traversing gear. A series of tests was undertaken to investigate these possibilities. Wires of various lengths were used in a variety of probe support configurations and in conjunction with several different window widths of the probability analyser. The required r.m.s. value was obtained in each case by a simple observation of the peak of the probability density, and to reduce the scatter the wires were calibrated before and after every run. Some of the measurements were repeated with the tungsten DISA wire in place of the usual Wollaston type. The r.m.s. longitudinal intensity at the centre of the wake was found to be reproducible within ± 2 % throughout; it therefore seems that, of the possibilities listed above, items (i) and (iii) can be discounted.

Item (ii) was investigated by plotting calibration curves using the power law suggested by Collis & Williams. The extracted small-signal sensitivity was indistinguishable from that obtained by using a King's law plot. In this connexion, it should be noted that the wires were calibrated over a range of 6 to 12 m/s, so the question of anomalous heat transfer at zero flow speed does not arise. Item (iv) includes two possibilities: either the low-frequency cut-off of the present

	Wake	Jet	Boundary layer
σ_0/y_0	0·21	0·22	0·17
$y_0\Sigma_0/\sigma_0$	2·8	3·1	2·6

TABLE 1. σ_0 is the standard deviation of the intermittency factor, y_0 is the distance of the half-intermittency point from the centre-plane or wall and Σ_0 is the r.m.s. interface slope. Sources: for the wake, the present measurements; for the jet and boundary layer, Townsend (1966, table 2).

equipment, about 0·1 Hz, may be lower than Townsend's or the high-frequency cut-off, 5 kHz, may be higher. To check the effect of low-frequency response, the r.m.s. intensity was measured directly with the DISA Random Signal Indicator & Correlator, which has a cut-off (-3 dB) at 3 Hz. The results were about 10 % lower than those obtained with the probability analyser, but still 20 % higher than Townsend's value. On the other hand, since the maximum frequency present in the flow was only a few kHz, it seems unlikely that the earlier constant-current system would miss a significant proportion of the turbulence energy as a result of inadequate high-frequency response.

To check item (v) some tests were carried out at a free-stream speed of 12 m/s, giving a Reynolds number closer to that used by Townsend. The ratio of the r.m.s. longitudinal intensity to the free-stream speed was found to be about 5 % higher than at 10 m/s, so the discrepancy is not a Reynolds-number effect. Item (vi) is unlikely in view of the good agreement of the mean velocity profiles, the almost perfect symmetry of the intermittency distribution about the centre-plane and the two-dimensionality of the wake over most of the width of the tunnel.

In spite of these and other tests, it has not been found possible to resolve the discrepancy in the measurements of turbulence intensity.

Possibly the most striking feature of the present experiments, taken as a whole, is that the disagreements with earlier measurements are in a direction which reduces the apparent difference between the wake and other plane flows. Table 1 illustrates this point. It would appear that the behaviour of the turbulence boundary in the wake resembles that in the jet and boundary layer more closely than has been previously supposed. Furthermore, if the present measurements of turbulence level are correct, the ratio of entrainment velocity to r.m.s. intensity is reduced, although the entrainment rate of the wake remains anomalously high.

5.2. *Summary of principal findings*

(i) The profile of intermittency factor is fitted by an error function and that of the burst rate by a Gaussian distribution, the standard deviations of the two curves being the same within the limits of experimental error. This implies that the modulus of the slope of the interface is uncorrelated with its instantaneous position.

(ii) The half-intermittency point is slightly further from centre of the wake and the standard deviation of the intermittency profile is considerably smaller than has been found in earlier wake measurements.

(iii) Although rather sensitive to imperfections in the turbulence detector, the experimental histograms representing the probability density for the time between bursts and the length of a burst are in agreement with a Poisson model of the intermittency signal, in which the probability of a front or back in an infinitesimal interval is simply proportional to the length of that interval. The profile of the standard deviation of the probability density for the time between bursts does not differ appreciably from the prediction of this model.

(iv) When allowance is made for experimental error, none of the above observations is inconsistent with a view of the turbulence boundary which regards its position as a normally distributed noise signal. The Poisson model used to fit the histograms is equivalent to the noise model except near the origin.

(v) The autocorrelation of the intermittency signal does not show pronounced periodicity, but owing to inadequate sample size definite conclusions cannot be drawn.

(vi) The conditional mean velocity is continuous at the interface. The gradient of the conditional mean is roughly constant within the turbulent zone for a given interface position, but the value of the slope depends on the position of the interface.

(vii) The probability densities for the longitudinal velocity component and its time derivative at the centre of the wake are similar to those found in grid turbulence. The turbulent zone probability density of velocity is skewed in the intermittent region, possibly owing to the effect of newly entrained fluid. The unconditional density is further skewed by the direct contribution from the irrotational zone.

(viii) The r.m.s. longitudinal turbulence intensity was found to be about 33% higher at the centre of the wake than indicated by the earlier measurements of Townsend. No explanation can be offered.

(ix) The longitudinal fluctuations in the irrotational zone agree with Phillips' (1955) theory even in the intermittent region. The virtual origin is near the centre-plane of the wake.

I wish to thank J. C. Mumford and R. J. Adrian for many useful discussions, Dr A. A. Townsend for the opportunity of working in his laboratory, and the Science Research Council for financial support.

REFERENCES

Batchelor, G. K. & Townsend, A. A. 1949 *Proc. Roy. Soc.* A **199**, 238.
Betchov, R. & Criminale, W. O. 1964 *Phys. Fluids*, **7**, 1920.
Bradbury, L. J. S. 1965 *J. Fluid Mech.* **23**, 31.
Bradshaw, P. 1967 *J. Fluid Mech.* **27**, 209.
Bruun, H. H. 1971 *J. Phys.* E, *Sci. Instrum.* **4**, 225.
Champagne, F. H., Sleicher, C. A. & Wehrmann, O. H. 1967 *J. Fluid Mech.* **28**, 153.
Collis, D. C. & Williams, M. J. 1959 *J. Fluid Mech.* **6**, 357.
Corrsin, S. 1963 *Handbuch der Physik*, vol. 8 (2), p. 524. Springer.
Corrsin, S. & Kistler, A. L. 1955 *N.A.C.A. Rep.* no. 1244.
Demetriades, A. 1968 *J. Fluid Mech.* **34**, 465.
Fiedler, H. & Head, M. R. 1966 *J. Fluid Mech.* **25**, 719.
Gartshore, I. S. 1966 *J. Fluid Mech.* **24**, 89.

GARTSHORE, I. S. 1967 *J. Fluid Mech.* **30**, 547.
GRANT, H. L. 1958 *J. Fluid Mech.* **4**, 149.
HESKESTAD, G. 1965 *J. Appl. Mech.* **32**, 721.
KLEBANOFF, P. S. 1955 *N.A.C.A. Rep.* no. 1247.
KOVASZNAY, L. S. G., KIBENS, V. & BLACKWELDER, R. F. 1970 *J. Fluid Mech.* **41**, 283.
MOBBS, F. R. 1968 *J. Fluid Mech.* **33**, 227.
NEE, V. W. & KOVASZNAY, L. S. G. 1969 *Phys. Fluids*, **12**, 473.
PERRY, A. E. & MORRISON, G. L. 1971 *J. Fluid Mech.* **47**, 765.
PHILLIPS, O. M. 1955 *Proc. Camb. Phil. Soc.* **51**, 220.
RICE, S. O. 1944 *Bell Syst. Tech. J.* **23**, 282.
RICE, S. O. 1945 *Bell Syst. Tech. J.* **24**, 46.
SANDBORN, V. A. 1959 *J. Fluid Mech.* **6**, 221.
SCHAPKER, R. L. 1966 *A.I.A.A. J.* **4**, 1979.
SNYDER, W. H. & MARGOLIS, D. P. 1967 *Phys. Fluids*, **10**, 963.
THOMAS, R. M. 1971 Ph.D. thesis, University of Cambridge.
TOWNSEND, A. A. 1947 *Proc. Roy. Soc.* A **190**, 551.
TOWNSEND, A. A. 1948 *Austr. J. Sci. Res.* **1**, 161.
TOWNSEND, A. A. 1949*a* *Proc. Roy. Soc.* A **197**, 124.
TOWNSEND, A. A. 1949*b* *Austr. J. Sci. Res.* **2**, 451.
TOWNSEND, A. A. 1956 *The Structure of Turbulent Shear Flow.* Cambridge University Press.
TOWNSEND, A. A. 1966 *J. Fluid Mech.* **26**, 689.
TOWNSEND, A. A. 1970 *J. Fluid Mech.* **41**, 13.
WYGNANSKI, I. & FIEDLER, H. 1969 *J. Fluid Mech.* **38**, 577.
WYGNANSKI, I. & FIEDLER, H. 1970 *J. Fluid Mech.* **41**, 327.